



## Enhancing PV Power Extraction Under Partial Shading Condition with Shade Dispersion Strategy

Parween R. Kareem<sup>1\*</sup>, Husniyah Jasim<sup>2</sup>, Fattah H. Hasan<sup>3</sup>, Sameer Algburi<sup>4</sup>

<sup>1</sup> Department of Electrical Technique, AL-Hawija Technical Institute /Northern Technical University

<sup>2</sup> Department of Electronic Technique, AL-Hawija Technical Institute /Northern Technical University

<sup>3</sup> Department of Mechanical Technique, AL-Hawija Technical Institute /Northern Technical University

<sup>4</sup> College of Engineering Technique, Al-Kitab University, Kirkuk, Iraq

### ARTICLE INFO

#### Article history:

Received November 3, 2023

Revised February 23, 2024

Accepted March 2, 2024

Available online March 6, 2024

#### Keywords:

PV array configurations

Partial Shading (PS)

Mismatch power losses

Fill Factor (FF)

Global maximum power point (GMPP)

Shade dispersion-based TCT(SD-TCT)

### ABSTRACT

Improving photovoltaic (PV) system efficiency is a popular field of research. Partial shading (PS) adversely impacts the solar system's output power, which considerably reduces the system's efficiency. As a result, this issue has been the subject of extensive investigation. When sunlight is blocked off of photovoltaic cells in a PV array, panel, or module, it is referred to as shading. Using a method that involves spreading shade throughout the PV array is one of the suggested fixes for this issue. This study compares the performance of a shade dispersion method to different PV array configurations under different partial shading circumstances, and it looks at how effective it is in a 3x3 PV system. MATLAB/Simulink is used for the evaluation. To achieve this, shade dispersion-based TCT (SD-TCT) under various shading scenarios has been compared to the current standard designs, which include series-parallel (SP), Honey-Comb (HC), Bridge-Linked (BL), and Total Cross-Tied (TCT). Based on the global maximum power (GMPP), mismatch power losses, fill factor (FF), percentage power losses (PL %), and PV system efficiency, the efficacy of the shade dispersion technique was assessed. For every partial shading condition (PSC) that was studied, the SD-TCT configuration outperforms the other setups in terms of fill factor and power loss.

## 1. Introduction

Nowadays, energy consumption of the world is Overcame by traditional, nonrenewable energy sources. Toxic and dangerous chemicals get released from These sources into the atmosphere. As a result, the climate and environment will be badly influenced leading to the worsening of global warming [1]; investigating alternative and renewable energy sources in immediate manner is important to secure environmental preservation, long-term sustainability, and fulfilment of the world's enormous energy demands [2-4]. photovoltaic energy systems, also known as PV systems, are a common type of renewable energy. The

thriving of photovoltaic technology can be attributed to various factors, including its environmental friendliness, the abundance of solar radiation, and its simple installation method on residential rooftops [5]. The photovoltaic effect, which is the process of turning solar photons into electricity by using semiconductors like silicon, is the basis for solar panel technology [6]. The factors that affect the effectiveness and performance of Systems the most are temperature, solar irradiation, and partial shading (PS) [7, 8].

The photovoltaic (PV) system's Maximum Power Point (MPP) have a great obstacle to be dodged which is the occurrence of PSC[9]. Partially shaded modules are the result of some

\* Corresponding author.

E-mail address: [preween\\_hwj@ntu.edu.iq](mailto:preween_hwj@ntu.edu.iq)

DOI: [10.24237/djes.2024.17104](https://doi.org/10.24237/djes.2024.17104)

This work is licensed under a [Creative Commons Attribution 4.0 International License](https://creativecommons.org/licenses/by/4.0/).



of a photovoltaic array's modules being partially shaded by surrounding structures, buildings, clouds, and other things. This leads to the production of multiple power points (MPPs), the greatest of which is the GMPP. It also greatly distorts the power- voltage(P-V) and current-voltage(I-V) curves. As a result, noticeable decrease in the maximum power that the PV array is capable of producing. Other sites refer to PV array's performance data, as Local Maximum Power Points (LMPPs) [10–12].

PSC effect in a solar photovoltaic array can be reduced by different methods and strategies. Such as using a variety of connectors. To do so, the PV array's module connections are modified from the traditional SP structure to a new arrangement, such as TCT, BL, or HC[7], [13]. when some of them are shaded from the sun, the amount of current that modules in a row generate is consequently reduced. As a result, regardless of any obstruction, multiple unique paths are created for the electric current to flow through [3]. Another method to lessen the effect of partial shadowing is to disperse the shadow uniformly throughout the displayed array. As long as the array's shadow pattern doesn't change, dispersion can be accomplished by moving PV modules around without breaking their connections[14]. Various algorithms are used to disperse partial shade in photovoltaic energy systems. Some common algorithms include the Particle Swarm Optimization (PSO) algorithm, the Genetic Algorithm (GA), and the Perturb and Observe (P&O) algorithm for Maximum Power Point Tracking (MPPT)mitigating partial shading effects[15].

The following tactics have been tested by several researchers in an attempt to raise the PV array's efficiency. The optimal energy harvesting under various shade conditions is described by Mayank Kumar [16] utilizing physical relocation and fixed column position modules with fixed electrical connections (PRFCPM-FEC). The algorithm is explained for  $m \times n$  modules under different shading conditions. The intended configuration is maintained while adjusting module placements without damaging electrical connections. Furthermore, a comparison is made between the suggested pattern arrangement, TCT, and actual

physical relocation of modules with fixed electrical connections (PRM-FEC). The array layout improves PSC performance, according to the results.

Under various shadowing situations, Kazerani et al. [17] investigated a variety of techniques, including SP, TCT, BL, half-reconfiguration photovoltaic arrays (HRPVA) and full reconfiguration photovoltaic arrays (FRPVA). The HRPVA composition produced the best outcomes.

For PV arrays of any size, Dhanup S. Pillai et al.[18] assessed a two-phase shadow dispersion technique. Due to its two separate phases, the two-phase approach utilized to relocate PV panels offers excellent shade dispersion. Four shade cases were compared to other approaches found in the literature to validate their involvement in physical relocation. Furthermore, a quantitative comparison between electrical reconfiguration (PSO), popular physical relocation (SuDoKu), and TCT connection procedures is provided for row current computation and bypass impact. According to the findings, the recommended two-phase approach can accomplish fill factors of 72% for short-wide scenarios, 62% for long-wide situations, 81% for short-narrow situations, and 75% for long-narrow conditions. Except for one pattern, the suggested method also produced a minimum power improvement of 700 W when compared to TCT in all shadow scenarios.

Sangram Bana and R.P. Saini [19] tested uniform and non-uniform shadowing on solar photovoltaic modules using various connection techniques. Array size experiments in different shadows were used to calculate the curves of solar system attributes. Different transmissivity meshes were used to create random shading patterns. Bypass diodes also impact the power production of photovoltaic systems. The final analysis identified the optimal module design under partial shadow and uniform insolation. As a conclusion the study recommend the partial shadowing the operation and design of solar systems.

Fabio Viola et al. [20] inspected the economic advantages of executing a reconfiguration system in photovoltaic plants to

promote efficiency and enhance power generation. cost-effectiveness of this system in different countries were evaluated with diverse incentive structures, giving consideration to factors like installation, shadow projections, incentives, and reconfiguration costs. Financial metrics like Net Present Value (NPV) and payback period are utilized to measure the usefulness of such an investment. The study concluded that the economic benefits of using a reconfiguration system for photovoltaic plants are considerable, especially taking into account the different incentive policies in various countries.

Possibility for static reconfiguration using Magic Su-Do-Ku were investigated by G. Madhusudanan and colleagues [21]. By the effective shadows spreading while maintaining TCT connections, the aim of this creative method was to maximize power generation and PV array performance enhancement in partially shadowed conditions. Consequently, determine the ideal circumstances for generating a substantial amount of electricity at the PV array's maximum power point (MPP), by examining different shading patterns. The outcome obtained under a variety of shading situations indicates the effectiveness and success of this methodology.

In a groundbreaking study, carried out by Suneel Raju Pendem and Suresh Mikkili [22] Simulations were carried to evaluate the performance of many PV array designs, including Series (S), SP, BL, and HC, under different shading patterns. Simulations were executed on 5\*5 PV array systems in MATLAB/Simulink. The HC design performed better than the others, regarding the outcomes, hence it is appropriate for standalone and on-grid PV systems with central inverters.

In this study, shade dispersion strategy-based TCT (SD-TCT) and various solar array configurations, were compared in terms of how well it works to improve the efficiency and performance of the photovoltaic system. The evaluation depends on the highest power produced, efficiency, FF, PL%, and the least amount of mismatch power losses.

## 2. Photovoltaic Array Modeling

Numerous scholars have previously offered a variety of methods, including single-, double-, and triple-diode models, for simulating PV cells. Figure 1 shows a simplified version of a photovoltaic (PV) cell with a single diode for clarity [21], a mathematical equation of a Photovoltaic solar cell module which characterizes the I-V characteristics is given by:

$$I_{ph} = \frac{[I_{SCR} + K_i(T - 298)]}{1000} * \lambda \tag{1}$$

$$I_{rs} = \frac{I_{SCR}}{[e^{(qV_{OC}/N_s KAT)} - 1]} \tag{2}$$

$$I_0 = I_{rs} \left[ \frac{T}{T_r} \right]^3 e^{\left[ \frac{qE_{go}}{BK} \left( \frac{1}{T_r} - \frac{1}{T} \right) \right]} \tag{3}$$

$$I = I_{ph} - I_0 \left( e^{\frac{q(V + IR_s)}{n_s AKT}} - 1 \right) - \left( (V + IR_s) / R_p \right) \tag{4}$$

where  $T_r$  and  $T$ : reference and operating temperature respectively.  $I_{ph}$ : represents the photo-generated current (A).  $I_0$ : PV module saturation current (A).  $A = B$ : ideality factor.  $k$ : Boltzmann constant.  $q$ : Electron charge.  $R_s$ : series resistance of a PV module.  $R_p$ : shunt resistance.  $I_{SCR}$ : the PV module short-circuit current at 25°C and 1000W/m<sup>2</sup>.  $K_i$ : short-circuit current temperature coefficient.  $\lambda$ : Solar irradiance.  $E_{go}$ : band gap of silicon.  $N_s$ ,  $N_p$ : number of series and parallel connected cells respectively

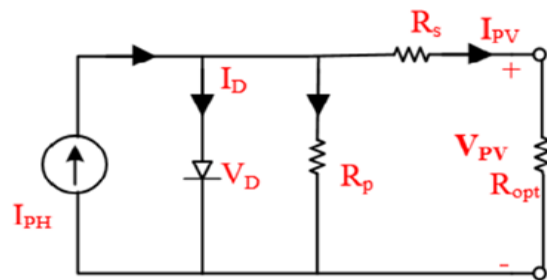


Figure 1. PV cell single-diode circuit [23]

Figure 2 represents the mathematical representation of a photovoltaic cell using MATLAB/ Simulink. Figure 3 depicts the fundamental block diagram of the system outlined in this study, which has been simulated using Matlab.



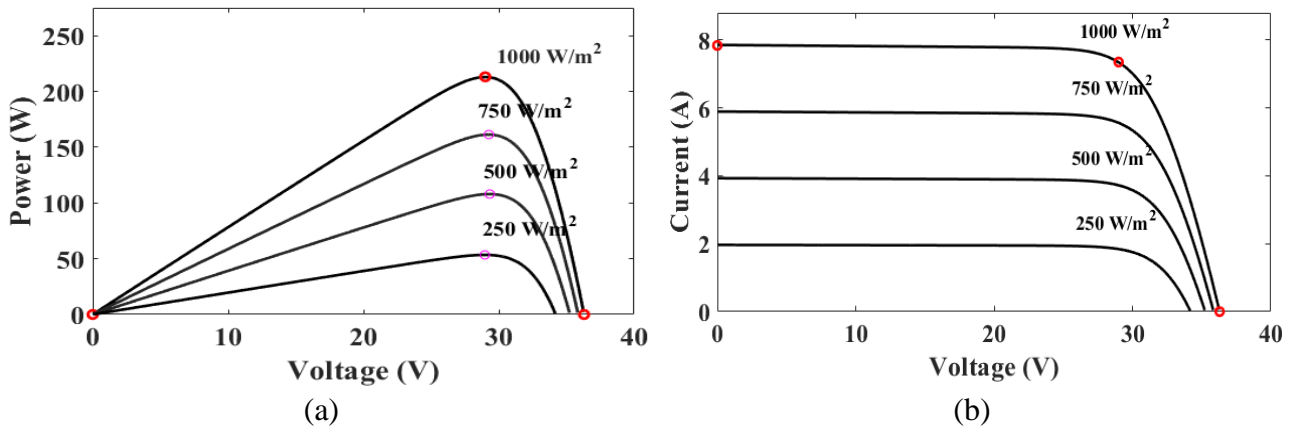


Figure 4. Different solar irradiance PV module characteristics (a) P-V Characteristics and (b) I-V Characteristics

### 3. PV Array Configurations

Solar power systems fall into two basic categories: standalone systems, which are typically utilized in rural and remote regions and have a power output of a few kilowatts, and grid-connected systems, which can provide the grid with many megawatts of power [14]. To meet the voltage and current requirements of the electrical network or the power requirements of the loads, solar panels must be assembled and connected to a photovoltaic (PV) array [5], [13]. To evaluate how well the proposed shade dispersion method works to lessen the effects of a partial shadow scenario, it needs to be compared to existing standard setups. With MATLAB/Simulink, four distinct configurations—the SP, HC, BL, and TCT—have been simulated. The P-V and I-V properties of the SD-TCT setup were then compared using these configurations in various partial shadow scenarios. Figure 5 displays every configuration utilized in this paper. Figure 5(a) displays the SP's blueprint, the first step in achieving the desired output voltage is to connect every module in series. Consequently, these series of connections must be combined in parallel. Three parallel series strings are created when PV modules are joined in groups of three using the CT arrangement. This configuration is comparable to an SP. However, as Figure 5(b) shows, series strings are also connected in

parallel at the end of each row. Figure 5(c) shows a graphic illustration of the BL setup. To be more precise, the bridging unit consists of four distinct parts. Connecting identical modules in parallel is the next step after connecting two modules in series within a circuit. Cross ties are employed to link the different bridges that comprise a network. In addition, Figure 5(d) displays the HC arrangement. The bridge's dimensions can be changed to provide an alternative configuration for the HC configuration, which is a modified version of the BL design [4]. In this paper, manually moving the solar panel while maintaining the electrical connections is the preferred method for shade dispersion. Thus, as shown in Figure 5(e), the Shade Dispersion Technique-Based TCT (SD-TCT) is presented. The TCT arrangement is used to create electrical linkages between the PV modules. On the other hand, all PV modules that are physically connected inside an array of PV modules in a series column string are those that belong to an odd-numbered row according to their electrical connection. The modules from even-numbered rows are grouped again after being arranged in a column with all the odd-numbered modules first, followed by the electrical connections. Additionally, the module linked in the first row of a given column moves a certain number of rows following each succeeding column in a sequential fashion.

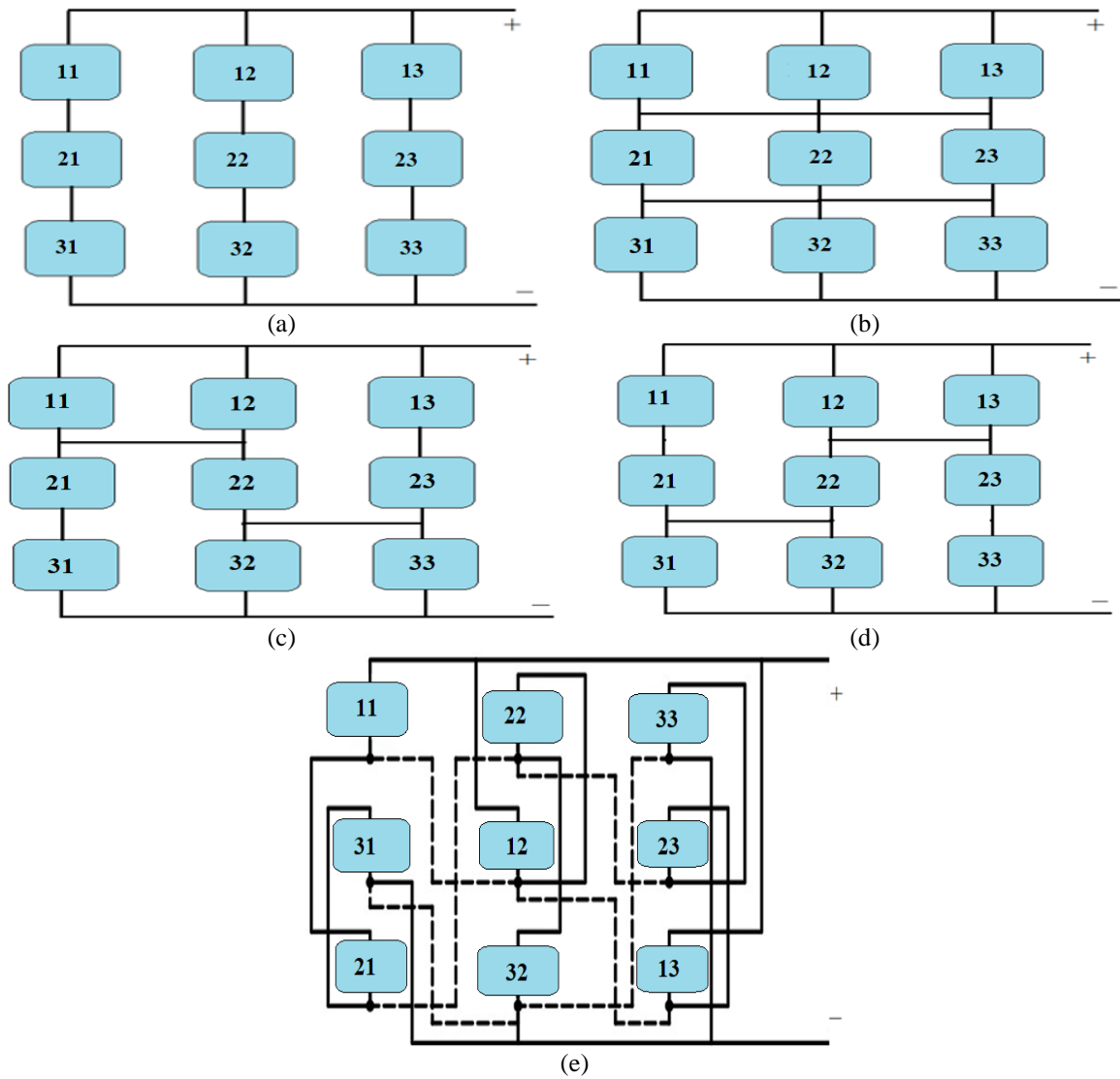


Figure 5. PV Module interconnection Styles; (a) SP; (b) TCT; (c) BL; (d) HC; (e) SD-TCT interconnections

#### 4. Results and discussion

The purpose of this study is to present simulation results for the five PV array topologies operating under various PSCs. Measured and compared across PV installations in MATLAB/SIMULINK simulations of different partial shade circumstances were GMPP, mismatching power losses, FF, and PL%. On a 3x3 PV array operating in PSCS mode, experiments were conducted to evaluate the effectiveness of various array configurations. To assess the PV system's

performance, the study exposed the solar modules to two different partial shade patterns:

The first pattern: Cases I, II, and III in Figure 6 represent what is thought to be progress on the leftmost modules (from top to bottom) where the moving shadow is seen.

The second pattern is represented by examples IV, V, and VI in Figure 6 and is interpreted as progress on the bottommost modules (from left to right).

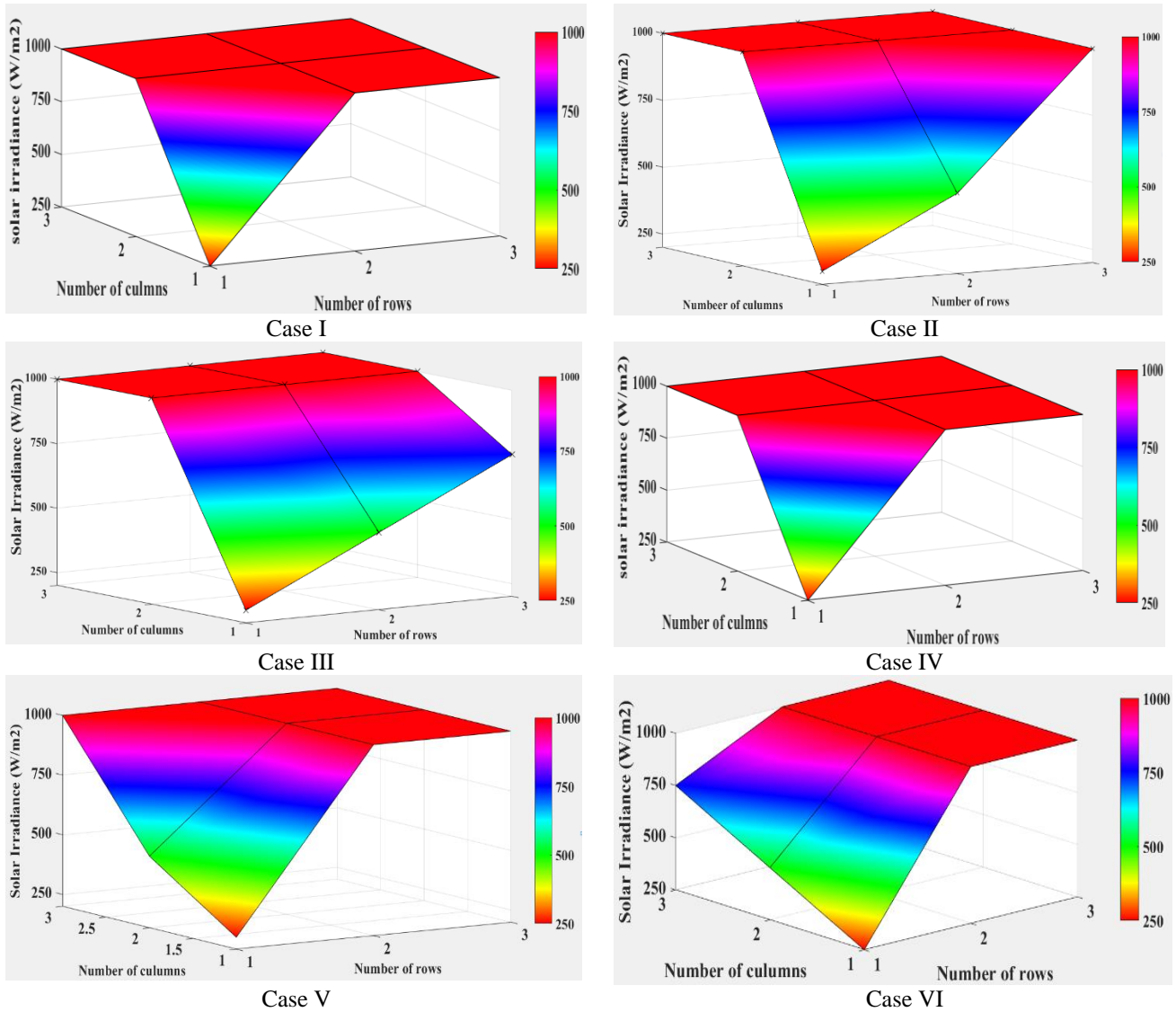


**Figure 6.** Partial shading patterns

Initially, to determine whether the HC, TCT, BL, and SD-TCT configurations reduce the amount of electricity produced under normal conditions, they must be contrasted with the conventional connection SP architecture without shade. The measured I-V and P-V characteristics of all possible PV array designs at the same operating conditions (1000 W/m<sup>2</sup> and 25°C) are displayed in Figures 7, where

Figure 7(a) represent I-V characteristics and Figure 7(b) represent I-V characteristics. Table 2 provides information on the maximum power output of a 3x3 solar array. All five array layouts have nearly identical maximum power levels, according to the research, and there is just one notable power peak. The simulation results of PV array configurations under shading cases are represented in Table 3.

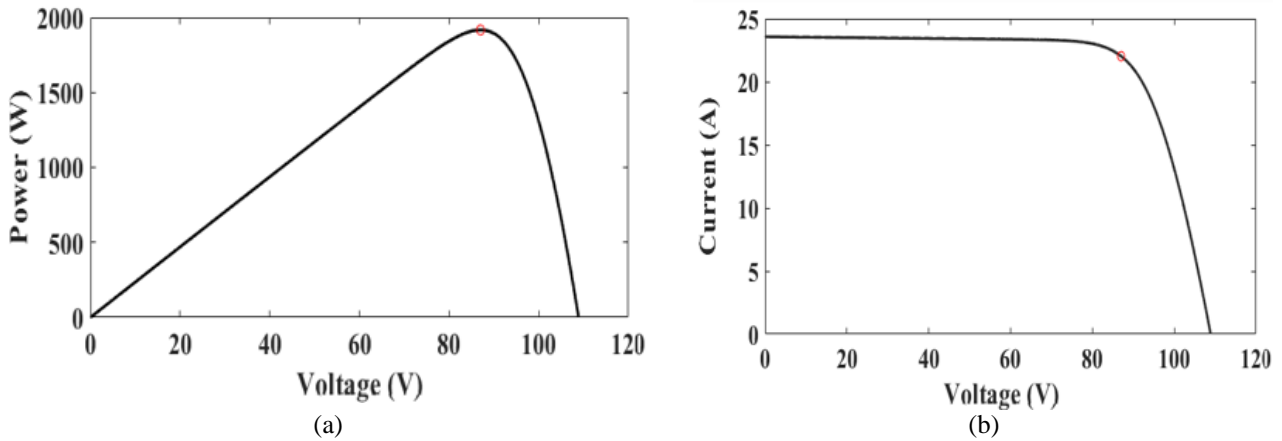


Figure 7. (a) P-V and (b) I-V curves of PV array configuration at STC

Table 2: Simulation results under uniform irradiance conditions

Configuration	Vo.c(V)	Is.c(A)	Vmpp(V)	Impp(A)	Pmax (W)	FF (%)
SP	108.8637	23.59322	87.0111	22.02497	1916.41664	0.746138889
TCT	108.8637	23.59322	87.0111	22.02497	1916.41664	0.746138889
BL	108.8637	23.59322	87.0111	22.02497	1916.41664	0.746138889
HC	108.8637	23.59322	87.0111	22.02497	1916.41664	0.746138889
SD-TCT	108.8637	23.59322	87.0111	22.02497	1916.41664	0.746138889

Table 3: Simulation results of shading cases

Cases	Confi.	Global Peak Parameter								
		Vo.c(V)	Is.c (A)	Vmax(V)	I <sub>max</sub> (A)	P <sub>max</sub> (W)	FF	Mismatch power losses	Percentage power losses	Efficiency %
Case I	SP	108.2829	23.593161	87.5919	16.531587	1448.0331	0.566803	468.38344	0.244405853	10.264515
	TCT	108.3192	23.593152	89.0439	16.607172	1478.7674	0.57864	437.64919	0.228368501	10.48237752
	BL	108.3192	23.593152	89.0439	16.607260	1478.7752	0.578643	437.64137	0.228364422	10.48243293
	HC	108.3918	23.593049	91.2945	17.164946	1567.0651	0.612783	349.35147	0.182294113	11.10828396
	SD-TCT	108.3918	23.593049	91.2945	17.164946	1567.0651	0.612783	349.35147	0.182294113	11.10828396
Case II	SP	107.9199	23.593105	58.8423	21.996210	1294.3075	0.508335	622.1090414	0.324620977	9.17481712
	TCT	107.9562	23.593049	57.354	22.006106	1262.1382	0.495536	654.2784246	0.341407192	8.946781522
	BL	107.9562	23.593049	57.354	22.006105	1262.1381	0.495536	654.278471	0.341407217	8.946781193
	HC	107.9925	23.593049	57.354	22.006105	1262.1381	0.495369	654.2784468	0.341407204	8.946781364
	SD-TCT	108.0651	23.592545	89.9877	17.106129	1539.3412	0.603774	377.0753524	0.196760634	10.91176071
Case III	SP	107.7384	23.593049	57.354	22.005853	1262.1236	0.496532	654.2929427	0.341414768	8.946678608
	TCT	107.7747	23.593049	57.354	22.005853	1262.1237	0.496364	654.2929206	0.341414757	8.946678765
	BL	107.7747	23.593049	57.354	22.005853	1262.1237	0.496364	654.2929363	0.341414765	8.946678654
	HC	107.811	23.593049	57.354	22.005853	1262.1237	0.496197	654.2929117	0.341414752	8.946678828
	SD-TCT	107.9562	21.626445	89.5158	17.083427	1529.2366	0.655001	387.1799678	0.202033295	10.84013322
Case IV	SP	108.2829	23.593161	87.5919	16.531587	1448.0331	0.566803	468.3834436	0.244405853	10.264515
	TCT	108.3192	23.593152	89.0439	16.607172	1478.7674	0.578640	437.6491948	0.228368501	10.48237752
	BL	108.3192	23.593152	89.0439	16.607260	1478.7752	0.578643	437.6413774	0.228364422	10.48243293
	HC	108.3918	23.593049	91.2945	17.164946	1567.0651	0.612782	349.3514707	0.182294113	11.10828396
	SD-TCT	108.3918	23.593049	91.2945	17.164946	1567.0651	0.612782	349.3514707	0.182294113	11.10828396
Case V	SP	108.0288	23.592992	87.5919	16.530227	1447.9139	0.568094	468.5026452	0.244468053	10.26367003
	TCT	108.0651	23.592714	89.0439	16.604882	1478.5635	0.579931	437.8531501	0.228474926	10.48093176
	BL	108.0651	23.592714	89.0439	16.604879	1478.5632	0.579931	437.8533989	0.228475056	10.48093
	HC	108.0651	23.592545	89.9877	17.106231	1539.3503	0.603778	377.0662918	0.196755906	10.91182493
	SD-TCT	108.0651	23.592546	90.024	17.099223	1539.3405	0.603774	377.0761389	0.196761044	10.91175513
Case VI	SP	107.7384	23.593049	57.354	22.005853	1262.1237	0.496532	654.2929287	0.341414761	8.946678708
	TCT	107.7747	23.593049	57.354	22.005853	1262.1237	0.496365	654.2929208	0.341414757	8.946678764
	BL	107.7747	23.593049	57.354	22.00585	1262.1237	0.496365	654.2929205	0.341414756	8.946678766
	HC	107.811	23.593049	57.354	22.005854	1262.1237	0.496198	654.292911	0.341414752	8.946678833
	SD-TCT	107.9562	21.626445	89.4795	17.090340	1529.2351	0.655000	387.1815088	0.202034099	10.8401223

The P–V characteristics of several PV array topologies under various partial shadowing scenarios are shown in Figure 8. Two maximum

power points (MPPs) are shown in the P-V curves of all designs in Figure 8(a). The GMPP of the BL and HC versions is 1478.7674W,

whereas the GMPP of the SP configuration is 1448.0332W. The maximum power of the TCT and SD-TCT configurations is 1567W.

The shading for case II is looked at in Figure 8 (b). Three MPPs and a GMPP are present in SD-TCT at 1539.341 W. In BL, HC, and TCT setups, two MPPs with a maximum power of 1262.138 W are seen; this is significantly more than the actual GMPP and results in increased shadowing. For the SP configuration, a single MPP with a maximum power of 1294.308 is discovered.

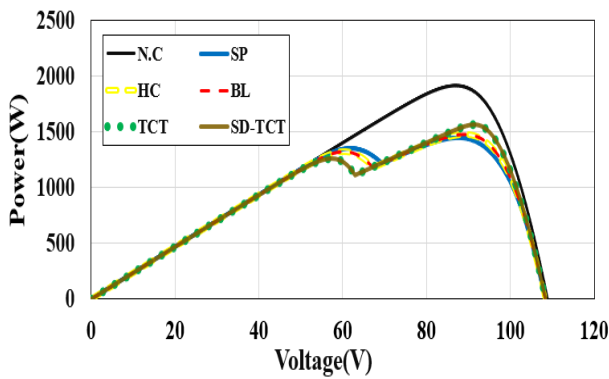
The P-V curves for the partial shadowing condition in instance III are shown in Figure 8(c). In this case, the curves for the SP, HC, BL, and TCT configurations are the same and have two MPPs with a maximum power output of 1262.124 W. In scenario 4, this value is acknowledged as the actual GMPP for the PSCs. Because of its distance from the GMPP, the LMPP may have a stronger shading impact. Three MPPs are detected for the SD-TCT configuration; two of them are LMPPs, while the third is a GMPP with a power value of 1529.237W.

The outcomes of instance I-V coincide with case I. Figure 8 (d) shows the P-V curves under the partial shadowing situation of case IV.

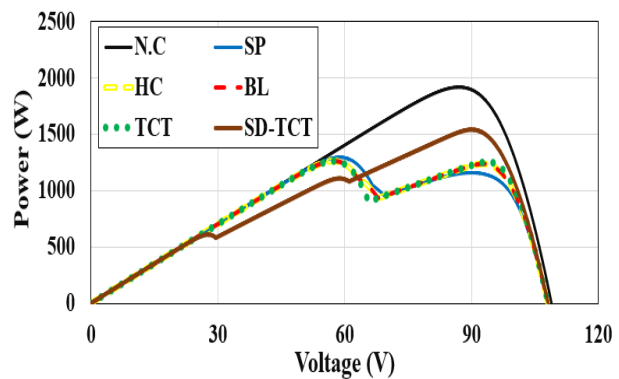
In Figure 8 (e), the P-V curves for case V are shown. The curves for the SP and BL configurations are the same, with three MPPs. The GMPP is determined to be around 1478 W. Because of its distance from the GMPP, the LMPP may have a greater shading impact. Two MPPs match the P-V curve for the HC and TCT arrangement; the GMPP, located at 1262.138W, is one of them, and the LMPP is the other. Three MPPs are detected for the SD-TCT configuration; two of them are LMPPs, and the third one, with a power value of 1539.341 W, is a GMPP.

Figure 8(f) displays the P-V curves for case VI's partial shadowing condition. The P-V curves for the SP, HC, BL, and TCT configurations are the same; two MPPs have emerged, and GMPP is discovered to be at 1262.124W. In the P-V curve for the SD-TCT configuration, three MPPs have emerged; two of them are LMPPs, and the third is GMPP, which is discovered to be at 1529.235W.

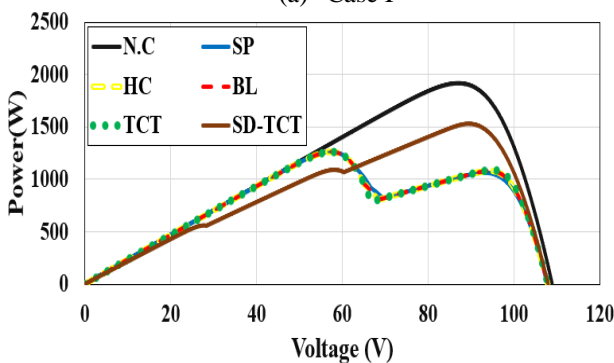
The GMPP is shown for several PV array topologies in Figure 9. It shows that when it comes to tracking the MPP under PSCs, the SD-TCT method works better than other configurations.



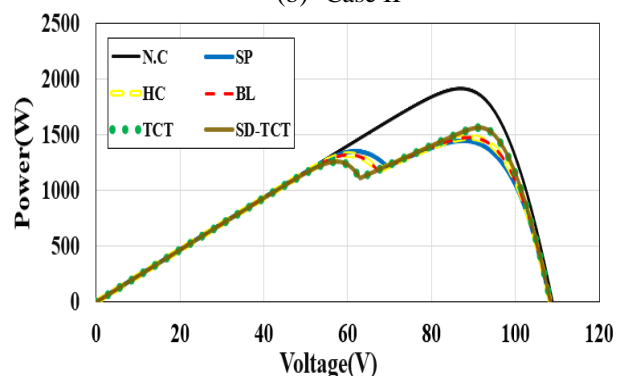
(a) Case I



(b) Case II



(c) Case III



(d) Case IV

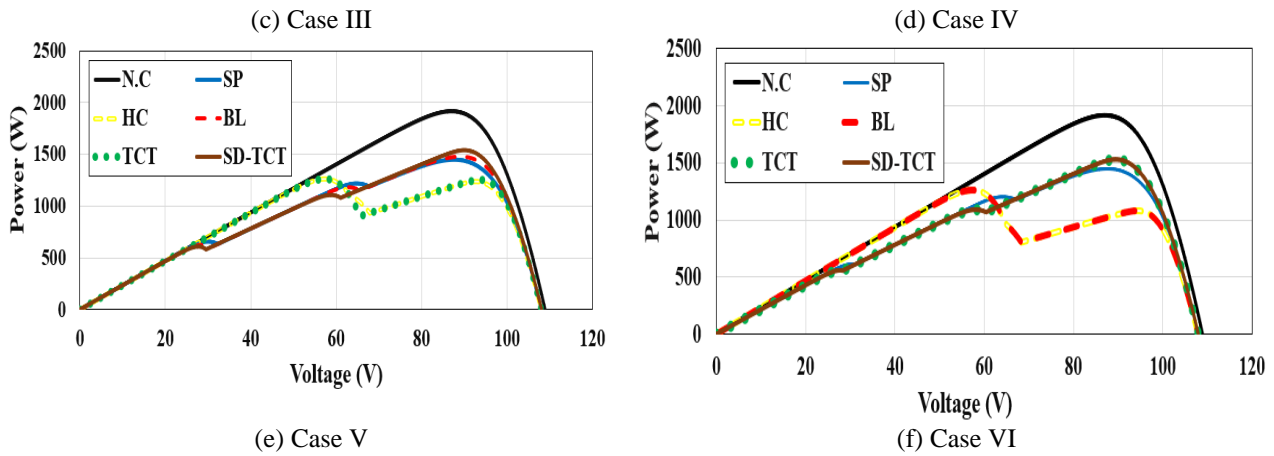


Figure 8. P-V Curve of PV array under shading pattern

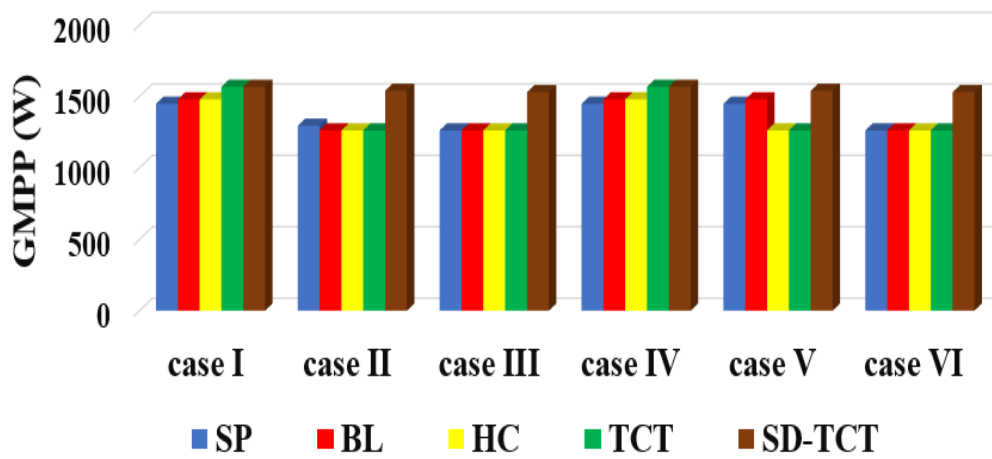


Figure 9. GMPP of various PV array configurations

Figure 10 uses bar graphs to display the fill factor of different PV array arrangements, while Figure 11 displays the power losses brought on by mismatches. It is observed that the SD-TCT

performs better and demonstrates good results in all scenarios examined in this research by lowering mismatch losses and raising the FF.

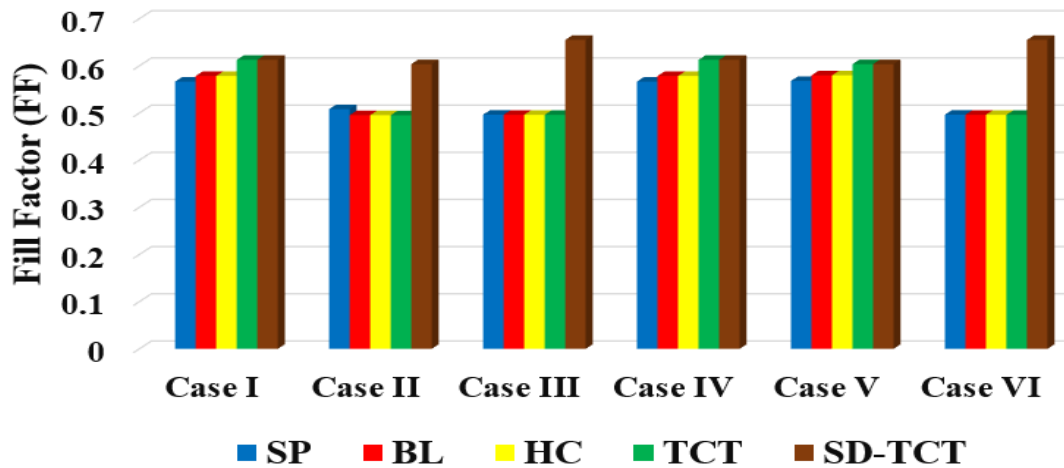


Figure 10. Fill factor of various PV array configurations

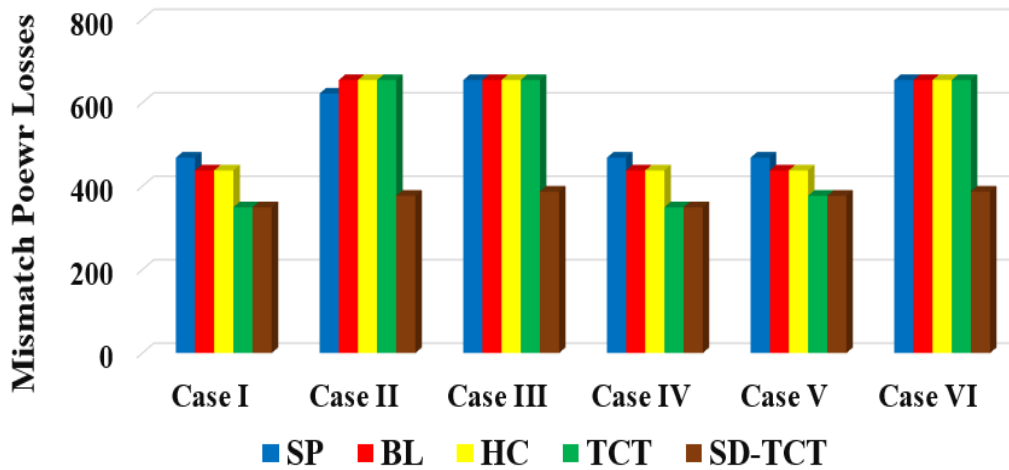


Figure 11. Mismatch power losses of various PV array configurations

Figure 12 displays bar graphs representing the percentage power losses (PL%) of the different PV array configurations. PL% is the ratio of the GMP obtained under unshaded conditions to the GMP obtained under shaded conditions. It is seen that the SD-TCT performs better than all other configurations and

demonstrates good results by lowering the percentage power losses in cases II, III, and VI. TCT and SD-TCT are equally effective in terms of percentage power losses in Cases I, IV, and V, while also outperforming the alternative design.

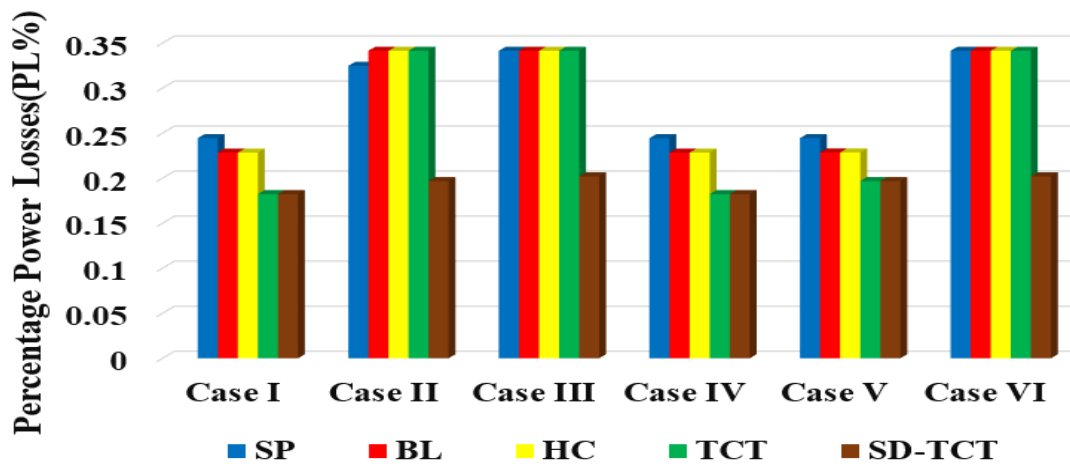


Figure 12. Percentage of Power Losses of various PV array configurations

Figure 13 displays bar graphs illustrating the efficiency of different PV array configurations. It is observed that in all instances examined in this study, the SD-TCT

consistently outperforms and demonstrates favourable outcomes by enhancing the efficiency of the PV system.

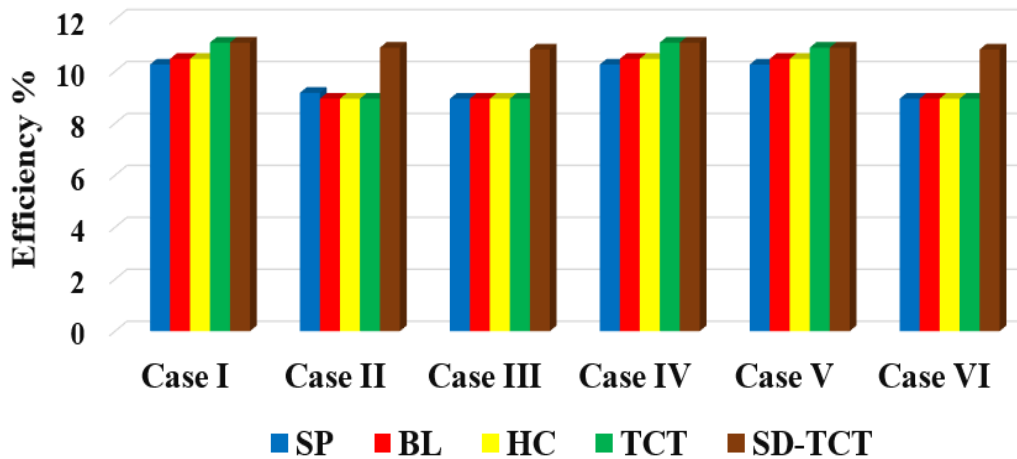


Figure 13. Efficiency of various PV array configurations

## 5. Conclusions

The SP, HC, BL, TCT, and SD-TCT PV array topologies, among others, have all been the subject of extensive research and analysis. On the above-specified setups, two different partial shade patterns for the solar modules have been investigated. The resulting metrics have been used to assess and contrast their performance, including GMPP, mismatch power loss, FF, and percentage power loss. The findings of the thorough simulation have been examined. Out of all the partial shading scenarios studied, the results show that SD-TCT exhibits the lowest power loss, maximum fill factor (FF), and best performance ratio. In the circumstances of partial shadowing that were studied, the efficiency of the photovoltaic energy system improved. Concerning examples I, II, III, IV, V, and VI, the shade dispersion technique specifically produced percentage improvements of 8%, 19%, 21%, 8%, 6%, and 21%, respectively. The SD-TCT method used in this research does not incur any additional economic costs, as the basic idea is based on changing the locations of solar panels within the photovoltaic system itself while maintaining electrical connections. Numerous studies have shown that PV array reconfiguration provides significant economic benefits, especially when taking into account the incentive programs offered in different countries. This underscores the importance of looking not only at technical improvements but also at regulatory and economic contexts when assessing the

feasibility and profitability of such initiatives [20]. It is proposed to apply this technique practically, to study the future obstacles and difficulties that it may face, and to propose the integration of shadow scattering technology with maximum power point tracking (MPPT) algorithms. The facility's visual appearance may alter as a result of the application of shadow dispersion technology, which may not always be desirable, particularly if the facility has historical or artistic significance. In some contexts, the technology may encounter technical and engineering constraints, such as the requirement for enough room to install systems. or the required engineering adjustments

## References

- [1] P. R. Kareem, "Performance of PV panel under shaded condition," *NTU Journal of Renewable Energy*, vol. 1, no. 1, pp. 22–29, 2020.
- [2] M. Kumar, K. P. Panda, J. C. Rosas-Caro, A. Valderrabano-Gonzalez, and G. Panda, "Comprehensive Review of Conventional and Emerging Maximum Power Point Tracking Algorithms for Uniformly and Partially Shaded Solar Photovoltaic Systems," *IEEE Access*, vol. 11, pp. 31778–31812, 2023.
- [3] L. F. L. Villa, D. Picault, B. Raison, S. Bacha, and A. Labonne, "Maximizing the power output of partially shaded photovoltaic plants through optimization of the interconnections among its modules," *IEEE Journal of Photovoltaics*, vol. 2, no. 2, pp. 154–163, 2012.

- [4] P. R. Kareem, S. Algburi, H. Jasim, and F. H. Hasan, "Optimal PV array configurations for partial shading conditions," *Indonesian Journal of Electrical Engineering and Computer Science*, vol. 32, no. 1, pp. 1–12, 2023.
- [5] B. Ö. Okan Bingöl, "Analysis and comparison of different PV array configurations under partial shading conditions," *Solar Energy*, vol. 160, no. July, pp. 336–343, 2018.
- [6] M. Saadsaoud, H. A. Abbassi, S. Kermiche, and M. Ouada, "Study of partial shading effects on photovoltaic arrays with comprehensive simulator for global MPPT control," *International Journal of Renewable Energy Research (IJRER)*, vol. 6, no. 2, pp. 413–420, 2016.
- [7] J. C. Teo, R. H. G. Tan, V. H. Mok, V. K. Ramachandaramurthy, and C. Tan, "Impact of partial shading on the P-V characteristics and the maximum power of a photovoltaic string," *Energies*, vol. 11, no. 7, 2018, doi: 10.3390/en11071860.
- [8] T. S. U. Vadivel, Srinivasan, Sridhar Ramasamy, Suresh Mikkili, Mominul Ahsan, Julfikar Haider, Md. Minarul Islam, "Hybrid Social Grouping Algorithm-Perturb and Observe Power Tracking Scheme for Partially Shaded Photovoltaic Array," *International Journal of Energy Research*, 2023.
- [9] A. Kovach and J. Schmid, "Determination of energy output losses due to shading of building-integrated photovoltaic arrays using a raytracing technique," *Solar Energy*, vol. 57, no. 2, pp. 117–124, 1996. doi: 10.1016/S0038-092X(96)00066-7.
- [10] A. Z. Yasser E. Abu Eldahab, Naggar H. Saad, "Enhancing the tracking techniques for the global maximum power point under partial shading conditions," *Renewable and sustainable energy reviews*, vol. 73, no. June, pp. 1173–1183, 2017.
- [11] H. B. Loubna Bouselhama, Mohammed Hajjia, Bekkay Hajji, "A new MPPT-based ANN for photovoltaic system under partial shading conditions Loubna," *Energy Procedia*, vol. 111, pp. 924–933, 2017.
- [12] E. Karatepe, M. Boztepe, and M. Çolak, "Development of a suitable model for characterizing photovoltaic arrays with shaded solar cells," *Solar Energy*, vol. 81, no. 8, pp. 977–992, 2007.
- [13] O. I. Andres Calcabrini, Raoul Weegink, Patrizio Manganiello, Miro Zeman, "Simulation study of the electrical yield of various PV module topologies in partially shaded urban scenarios," *Solar Energy*, vol. 225, no. July, pp. 726–733, 2021.
- [14] A. L. M. Khaleel, Nibras A.J., "Solar Photovoltaic Array Reconfiguration for Reducing Partial Shading Effect," *Asian Journal For Convergence In Technology (AJCT)*, vol. VII, no. II, pp. 114–120, 2021.
- [15] T. Alves, J. P. N. Torres, R. A. Marques Lameirinhas, and C. A. F. Fernandes, "Different techniques to mitigate partial shading in photovoltaic panels," *Energies*, vol. 14, no. 13, 2021.
- [16] M. Kumar, "Enhanced Solar PV Power Generation Under PSCs Using Shade Dispersion," *IEEE Transactions on Electron Devices*, 67(10), pp.4313-4320, 2020,
- [17] M. Z. S. El-Dein, M. Kazerani, and M. M. A. Salama, "Novel configurations for photovoltaic farms to reduce partial shading losses," *IEEE Power and Energy Society General Meeting*. 2011.
- [18] J. P. R. Dhanup S. Pillai, N. Rajasekar and V. K. Chinnaiyan, "Design and testing of two phase array reconfiguration procedure for maximizing power in solar PV systems under partial shade conditions (PSC)," *Energy conversion and management*, vol. 178, no. December, pp. 92–110, 2018.
- [19] S. Bana and R. P. Saini, "Experimental investigation on power output of different photovoltaic array configurations under uniform and partial shading scenarios," *Energy*, vol. 127, pp. 438–453, 2017.
- [20] F. Viola, P. Romano, R. Miceli, C. Spataro, G. Schettino, and F. Fanto, "Economic benefits of the use of a PV plants reconfiguration systems," *International Conference on Renewable Energy Research and Applications (ICRERA) 2015*, vol. 5, pp. 1654–1658, 2015.
- [21] G. Madhusudanan, N. Rakesh, S. Senthil Kumar, and S. Sarojini Mary, "Solar photovoltaic array reconfiguration using Magic Su-Do-Ku algorithm for maximum power production under partial shading conditions," *International Journal of Ambient Energy*, vol. 43, no. 1, pp. 1204–1215, 2022.
- [22] S. R. Pendem and S. Mikkili, "Modeling, simulation, and performance analysis of PV array configurations ( Series, Series-Parallel, Bridge-Linked, and Honey-Comb ) to harvest maximum power under various Partial Shading Conditions," *International journal of green energy*, vol. 00, no. 00, pp. 1–18, 2018.
- [23] P. R.Kareem, "Simulation of the Incremental Conductance Algorithm for Maximum Power Point Tracking of Photovoltaic System Based On Matlab," *Diyala Journal of Engineering Sciences*, vol. 12, no. 1, pp. 34–43, 2019, doi: 10.24237/djes.2019.12105.